4350 *Chem. Mater.* **2009,** *21,* 4350–4352
DOI:10.1021/cm902037w

CHEMISTRY OF
MATERIALS
Communication

Field-Effect Transistors Based on Tetraphenyldipyranylidenes and the Sulfur Analogues

Altan Bolag, Masashi Mamada, Jun-ichi Nishida, and Yoshiro Yamashita*

Department of Electronic Chemistry, Interdisciplinary Graduate School of Science and Engineering, Tokyo Institute of Technology, Nagatsuta, Midori-ku, Yokohama 226-8502, Japan

Received July 7, 2009
Revised Manuscript Received August 16, 2009

Organic field-effect transistors (OFETs) based on organic semiconductors have attracted much attention because of the applications such as flat-panel displays, electronic papers, and chemical sensors and because they have advantages of low cost, large-area fabrication, and fexibility.[1] Typical p-type semiconductors are acenes such as pentacene,[2] heterocyclic oligomers such as thiophene oligomers,[3] and tetrathiafulvalenes (TTFs).[4] Some of them exhibit higher hole mobilities than amorphous Si ($\sim$1.0 cm^2/(V s)).[5] Development of new π-electron systems for semiconductors is still very important for the progress of this field to explore new materials as well as to investigate relationship between structure and properties. We have now focused on 2,2′,6,6′-tetraphenyldipyranylidene (Ph$_4$DP) **1a** and the sulfur analogue (Ph$_4$DTP) **2a**[6] as new p-type semiconductors because they have the following advantages. First, they have an isoelectronic structure with TTF and the cation and dication states are stable.[7] Actually they have been used as electron donors to afford organic conductors like TTF.[8] Second, they have highly extended π-conjugation systems, which are favorable for strong intermolecular interactions, leading to high carrier mobilities. Third, the preparation method is very simple and substituents can be easily introduced. Finally, they have intense absorption in the visible region, which leads to a possibility of application to semiconductors for solar cells. However, they have never been used as semiconductors for FETs. We report herein the synthesis, physical properties, crystal structures, and their first FET performances.

Ph$_4$DP, Ph$_4$DTP, and the derivatives **1c**, **1h**, and **2b** are known compounds.[6,9] The derivatives **1b** and **1d**−**1g** are new compounds and were synthesized by the similar methods[10] to those for Ph$_4$DP and Ph$_4$DTP (Scheme 1). These compounds were purified by sublimation several times or recrystallization and characterized by mass spectrometry and elemental analysis.

The UV−vis absorption spectra in dichloromethane showed intense absorptions in the visible region because of the extended π-conjugation. The HOMO−LUMO energy gaps were estimated from the end absorptions. The halogen derivatives showed larger HOMO−LUMO energy gaps than **1a**. On the other hand, the alkyl derivatives **1f**−**1h** did not change the HOMO−LUMO energy gaps significantly. The absorption maxima of the sulfur analogues **2a** and **2b** were observed at longer wavelengths than those of **1a** and **1b**. This is considered to be attributed to the more polarized and less electronegative sulfur atom.

The electrochemical measurements of these compounds were performed in DMF. The cyclic voltammograms exhibited two oxidation waves and no reduction wave was observed. The redox potentials of **1d** and **1e** could not be measured because of the low solubility. The first oxidation potential of Ph$_4$DP is lower than that of TTF, indicating that Ph$_4$DP has a higher electron-donating ability than

---

*Corresponding author.

(1) (a) Newman, C. R.; Frisbie, C. D.; Da Silva Filho, D. A.; Brédas, J.-L.; Ewbank, P. C.; Mann, K. R. *Chem. Mater.* **2004**, *16*, 4436. (b) Amanda, R. M; Jean, M. J. F. *Chem. Rev.* **2007**, *107*, 1066. (c) Jana, Z.; Henning, S. *Chem. Rev.* **2007**, *107*, 1296. (d) Forrest, S. R.; Thompson, M. E. *Chem. Rev.* **2007**, *107*, 923.

(2) (a) Swartz, C. R.; Parkin, S. R.; Bullock, J. E.; Anthony, J. E.; Mayer, A. C.; Malliaras, G. G. *Org. Lett.* **2005**, *7*, 3163. (b) Hajlaoui, M. E.; Garnier, F.; Hassine, L.; Kouki, F.; Bouchriha, H. *Synth. Met.* **2002**, *129*, 215. (c) Roy, V. A. L.; Zhi, Y. G.; Xu, Z. X.; Yu, S. C.; Chan, P. W. H.; Che, C. M. *Adv. Mater.* **2005**, *17*, 1258.

(3) (a) Yoon, M. H.; DiBenedetto, S. A.; Facchetti, A.; Marks, T. J. *J. Am. Chem. Soc.* **2005**, *127*, 1348. (b) Ando, S.; Murakami, R.; Nishida, J.; Tada, H.; Inoue, Y.; Tokito, S.; Yamashita, Y. *J. Am. Chem. Soc.* **2005**, *127*, 14996. (c) Jones, B. A.; Ahrens, M. J.; Yoon, M.-H.; Facchetti, A.; Marks, T. J.; Wasielewski, M. R. *Angew. Chem., Int. Ed.* **2004**, *43*, 6363.

(4) (a) Mas-Torrent, M.; Rovira, C. *J. Mater. Chem.* **2006**, *16*, 433. (b) Mas-Torrent, M.; Hadley, P. *Appl. Phys. Lett.* **2005**, *86*, 012110. (c) Naraso; Nishida, J.; Kumaki, D; Tokito, S.; Yamashita, Y. *J. Am. Chem. Soc.* **2006**, *128*, 9598. (d) Naraso; Nishida, J.; Ando, S; Yamaguchi, J.; Itaka, K.; Koinuma, H.; Tada, H.; Tokito, S.; Yamashita, Y. *J. Am. Chem. Soc.* **2005**, *127*, 10142.

(5) (a) Goldmann, G.; Haas, S.; Krellner, C.; Pernstich, K. P.; Gundlach, D. J.; Batlogg, B. *J. Appl. Phys.* **2004**, *96*, 2080. (b) Kelley, T. W.; Boardman, L. D.; Dunbar, T. D.; Muyres, D. V.; Pellerite, M. J.; Smith, T. P. *J. Phys. Chem. B* **2003**, *107*, 5877. (c) Briseno, A. L.; Mannsfeld, S. C. B.; Ling, M. M.; Liu, S.; Tseng, R. J.; Reese, C.; Roberts, M. E.; Yang, Y.; Wudl, F.; Bao, Z. *Nature*. **2006**, *444*, 913. (d) Podzorov, V.; Menard, E.; Borissov, A.; Kiryukhin, V.; Rogers, J. A.; Gershenson, M. E. *Phys. Rev. Lett.* **2004**, *93*, 086602. (e) Menard, E.; Podzorov, V.; Hur, S.-H.; Gaur, A.; Gershenson, M. E.; Rogers, J. A. *Adv. Mater.* **2004**, *16*, 2097. (f) Mas-Torrent, M; Durkut, M; Hadley, P; Ribas, X; Rovira, C. *J. Am. Chem. Soc.* **2004**, *126*, 984.

(6) Reynolds, G. A.; Chen, C. H.; Van Allan, J. A. *J. Org. Chem.* **1979**, *44*, 4456.

(7) Hünig, S; Garner, B. J.; Ruider, G.; Schenk, W. *Liebigs Ann. Chem.* **1973**, 1036.

(8) (a) Dmitri, V.; Rimma, N.; Natal'ya, V. B; Evgeniya, I. Y; Shul'ga, Yury M.; Aleksey, L. L.; Viktor, N. S.; Boris, P. T. *J. Mater. Chem.* **2000**, *10*, 803. (b) Starodub, V. A.; Gluzman, E. M.; Golovkina, I. F.; Tsyguleva, O. M. *Sov. J. Chem. Phys.* **1982**, 291. (c) Viruela-Martin, R.; Viruela-Martin, P. M.; Orti, E. *J. Chem. Phys.* **1992**, *96*, 4474. (d) Strzelecka, H.; Schoenfelder, W. *Mol. Cryst. Liq. Cryst.* **1979**, *52*, 307.

(9) (a) Gionis, V.; Fugnitto, R.; Meyer, G.; Strzelecka, H.; Dubois, J. C. *Mol. Cryst. Liq. Cryst.* **1982**, *90*, 153. (b) Strzelecka, H.; Gionis, V.; Rivory, J.; Flandrois, S. *J. Phys., Paris* **1982**, 1201. (c) Es-Seddiki, S.; Hakiki, M.; Le Coustumer, G.; Mollier, Y.; Regnault Du Mottier, C.; Sauve, J. P *Bull. Soc. Chim. Fr.* **1984**, *5*−*6*, 241.

(10) (a) Reynold, G. A.; Chen, C. H. *J. Heterocycl. Chem.* **1981**, *18*, 1235. (b) Giancarlo, D.; Gianfranco, E. *Synthesis* **1985**, *8*, 789.

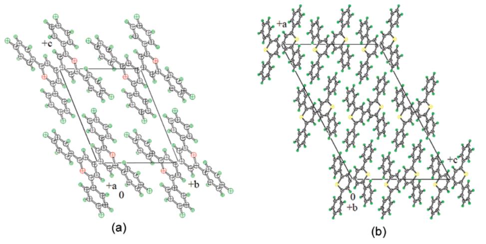

Figure 1. Packing structure of (a) **1b** along the *a* axis and (b) **2a** along the *b* axis.

Scheme 1. Synthesis of Compounds 1a−1h, 2a, and 2b[a]

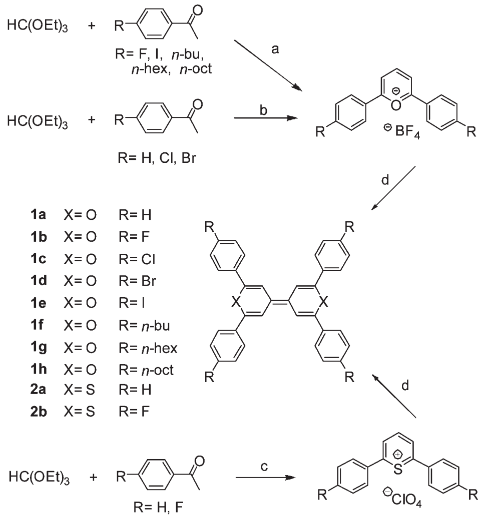

[a] Reagents: (a) BF_3−$O(C_2H_5)_2$; (b) HBF_4, 48%; acetic anhydride; (c) H_2S; $HClO_4$, 70%; acetic anhydride; (d) $(C_4H_9)_3P$; $EtNH(i\text{-}Pr)_2$; **1a**, 63%; **1b**, 43%; **1c**, 36%; **1d**, 20%; **1e**, 25%; **1f**, 72%; **1g**, 23%; **1h**, 20%; **2a**, 60%; **2b**, 74%.

TTF. Introduction of halogen groups decreases the HOMO levels, resulting in higher oxidation potentials. On the other hand, introduction of alkyl groups increases the HOMO levels leading to the lower oxidation potentials. The first oxidation potentials of **2a** and **2b** are a little higher than those of **1a** and **1b**. This may be related to the less planar structure of **2a** compared to **1a**. The second oxidation potentials of **2a** and **2b** were lower than those of **1a** and **1b** because of the lower Coulomb repulsion in the sulfur compounds.

To investigate their molecular structures and intermolecular interactions in the solid state, we carried out single-crystal structure analysis. The crystal structures of **1a** and **2a** were already reported.[11] For **2a**, we got a single-crystal structure that is different from the reported data. The single crystals of **1b** and **2a** were obtained by sublimation. The molecules of **1b** have a face-to-face packing along the *a* axis. The phenyl rings are twisted to the pyran ring with dihedral angles of 10.13 and 7.23°, which are similar to those of **1a** (9.95° and 7.41°). The interplanar distance between the molecules in the column is 3.037 Å. The molecule of **2a** is a little deformed, where the phenyl rings are twisted to the thiopyran ring with dihedral angles of 17.66 and 13.57°, which are larger than those in **1a**. These are different from the reported data (12.5 and 8.2°), where the crystal belongs to a different space group. The molecules pack in a face-to-face manner to form a column along the *b* axis. The interplanar distance between the molecules in the column is 3.399 Å, which is longer than that of **1b**.

Table 1. UV Absorptions[a] and Oxidation Potentials[b]

compd	λ_{max} (nm)	λ_{edge} (nm)	E_{gap} (eV) [c]	E^1_{ox} (V)	E^2_{ox} (V)
1a	273, 457	612	2.02	0.24	0.51
1b	265, 447	551	2.25	0.29	0.54
1c	280, 467	569	2.18	0.32	0.59
1d	277, 465	570	2.17		
1e	283, 466	570	2.17		
1f	279, 458	621	2.00	0.14	0.48
1g	279, 459	626	1.98	0.20	0.47
1h	279, 459	620	2.00	0.22	0.50
2a	263, 474	625	1.98	0.31	0.47
2b	258, 460	567	2.19	0.32	0.47

[a] In CH_2Cl_2. [b] In DMF, 0.1 M $n\mathrm{Bu_4NPF_6}$, Pt electrode, scan rate 100 mV/s, V vs SCE. [c] Obtained from the end absorptions.

Table 2. FET Characteristics of Compounds 1a−1h, 2a, and 2b[a]

compd	T_{sub} (°C)	surface	mobility ($\mathrm{cm^2V^{-1}s^{-1}}$)	on/off ratio	threshold (V)
1a	r.t	HMDS	1.9×10^{-2}	4×10^3	−0.8
	80	HMDS	5.0×10^{-2}	3×10^2	−1.7
	r.t	OTS	1.2×10^{-2}	3×10^3	−1.2
1b	r.t	HMDS	3.9×10^{-4}	1×10^5	−8.0
	80	HMDS	7.9×10^{-4}	2×10^5	−8.9
1c	r.t	HMDS	1.9×10^{-5}	1×10^3	−2.3
	80	HMDS	6.9×10^{-5}	2×10^3	−11
1d	r.t	HMDS	4.0×10^{-5}	4×10^4	−9.5
	80	HMDS	5.0×10^{-5}	2×10^4	−11
1e	r.t	HMDS	1.9×10^{-4}	3×10^2	−17
	50	HMDS	3.7×10^{-4}	5×10^2	−4.2
1f	r.t	HMDS	1.0×10^{-4}	2×10^3	−1.1
1g	r.t	HMDS	3.8×10^{-7}	3×10^3	−4.8
1h	r.t	HMDS	3.8×10^{-7}	40	−13
2a	r.t	HMDS	5.3×10^{-2}	4×10^4	−7.2
	80	HMDS	2.7×10^{-2}	4×10^4	−17
	r.t	OTS	9.7×10^{-2}	1×10^5	−9.2
2b	r.t	HMDS	1.4×10^{-4}	8×10^3	−0.5

[a] FETs were fabricated on Si/SiO$_2$. L/W = 25 μm/294 mm, Au electrode. SiO$_2$, 300 nm thick; semiconducting layer, 50 nm thick. The FET measurements were carried out in vacuum.

The FET devices were fabricated with bottom contact configuration and all of the compounds showed p-type FET characteristics in a vacuum (1×10^{-5} Pa). The FET performances are summarized in Table 2. The hole mobility of **1a** was 1.9×10^{-2} cm^2/(V s) with a low threshold voltage of −0.8 V, on an HMDS treatment substrate at the substrate temperature of 25 °C. On the other hand, the mobility of **2a** was a little higher than that of **1a**. The OTS treated film showed a mobility of 0.1 cm^2/(V s) and the on/off ratio was 1×10^5. However, neither of them was stable in air. Thus, the FET behavior of **1a** disappeared soon when exposed to air. **2a** showed better air stability. Mobility of **2a** decreased 1 order of magnitude when exposed to air in 10 min. Introduction of the halogen groups decreased the mobility. With an increase of the size of halogen atom, the mobility decreased gradually except for iodine. Compared with **1a**, on/off current ratios

---

(11) (a) Par, D. C.; J. Gaultieretc, H. *Acta Crystallogr., Sect. B* **1982**, *38*, 1629. (b) Henry, R. L.; Douglasl, L. S. *Acta Crystallogr., Sect. B* **1980**, *36*, 986.

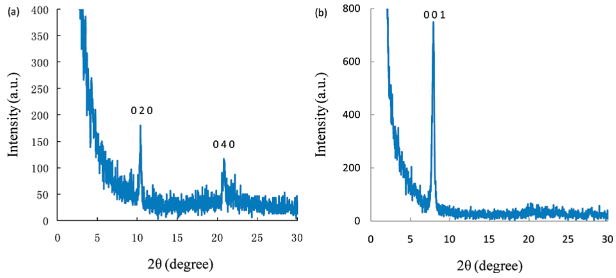

Figure 2. XRD of films deposited at room temperature for (a) **1a** and (b) **1b** on the HMDS treatment substrate.

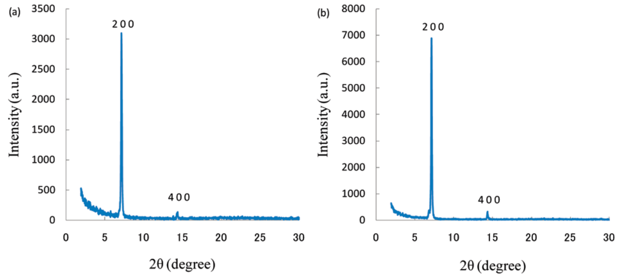

Figure 3. XRD patterns of **2a** films with the treatment of (a) HMDS and (b) OTS.

of compounds **1b** and **1d** became larger because of the lower off-current, which was caused by their increased ionization potentials measured by cyclic voltammograms (the oxidation potentials are higher than that of **1a**) as shown in Table 1. Table 2 also shows that the mobilities of **1a-e** could be improved by preparing films at the substrate temperature of 80 or 50 °C. This may be due to the smooth film growth or larger grain size at the higher substrate temperatures. Introduction of the alkyl groups into Ph_4DP decreased the mobility. Along with an increase in the alkyl chain length, the mobility decreased gradually.

In order to investigate the morphologies of the films, the films of these compounds deposited on the SiO_2/Si substrate were evaluated by X-ray diffraction (XRD) in a reflection mode. Figure 2 shows the XRD patterns of **1a** and **1b** films. For **1a**, the *d*-spacing obtained from the first reflection peak ($2\theta = 10.4°$) was 0.85 nm. Since the molecular length of **1a** obtained from the X-ray structure analysis is 1.06 nm, **1a** molecules are considered to have ca. 37° declining orientation on the substrate.

For compound **1b**, the *d*-spacing obtained from the reflection peak ($2\theta = 7.96°$) was 1.11 nm. Since the molecular length of **1b** obtained from the single-crystal X-ray analysis is 1.11 nm, the molecules of **1b** are considered to stand on the substrate perpendicularly. This is an ideal molecular arrangement on the substrate for charge transport. Figure 3 shows the XRD patterns of **2a** films on the HMDS and OTS treated substrates. Sharp reflections were observed in both films. The intensity of the first peak deposited on the OTS treated substrate increases more than twice compared to the film deposited on HMDS treated SiO_2. This observation suggests that the crystallinity increases on the OTS treatment. The *d*-spacing obtained from the reflection peak ($2\theta = 7.18°$) is 1.23 nm and the molecular length of **2a** obtained from the X-ray structure is 1.22 nm. This fact implies that the molecules are perpendicular to the dielectric surface.

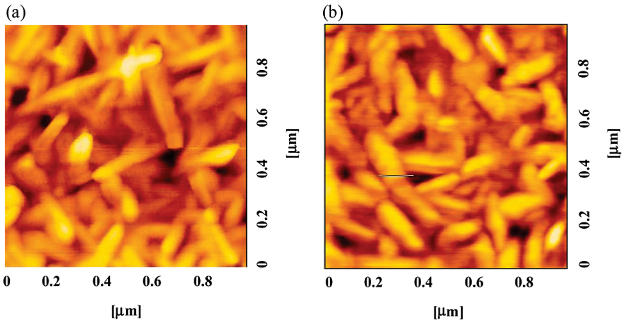

Figure 4. AFM images of the thim films of (a) **1a** and (b) **2a** (HMDS treatment).

Figure 4 shows the atomic-force microscopy (AFM) images of vacuum-deposited films of **1a** and **2a**. Large grains are observed in both the films. The grains in the film **2a** are more densely packed, leading to the higher mobility of **2a**.

In summary, tetraphenyldipyranylidene **1a** and its derivatives were used as organic semiconductors of OFETs for the first time. The parent compound **1a** and its sulfur analogue **2a** afforded good performance p-type FETs. The sulfur compound **2a** showed a better performance than **1a** because of the higher crystallinity. Halogen substituents and alkyl groups were introduced to the phenyl group of **1a** to increase the stability and solubility.

Acknowledgment. This work is supported by a Grant-in-Aid for Scientific Research (19350092) from the Ministry of Education, Culture, by Sports, Science and Technology, Japan, by Mizuho Foundation for the Promotion of Sciences, and by the Global COE program "Education and Research Center for Emergence of New Molecular Chemistry".

Supporting Information Available: Synthesis, absorption spectra, CVs, device fabrications, I_d versus V_d and I_d versus V_g characteristics of **1a** and **2a** (PDF); X-ray crystallographic data for **1b** and **2a** (CIF). This material is available free of charge via the Internet at http://pubs.acs.org.